Projection of Climate Change onto Modes of Atmospheric Variability

DÁITHÍ A. STONE AND ANDREW J. WEAVER

School of Earth and Ocean Sciences, University of Victoria, Victoria, British Columbia, Canada

RONALD J. STOUFFER

NOAA/Geophysical Fluid Dynamics Laboratory, Princeton University, Princeton, New Jersey

(Manuscript received 11 August 2000, in final form 26 December 2000)

ABSTRACT

Two possible interpretations of forced climate change view it as projecting, either linearly or nonlinearly, onto the dominant modes of variability of the climate system. An evaluation of these two interpretations is performed using annual mean sea level pressure (SLP) and surface air temperature (SAT) fields obtained from integrations of the Geophysical Fluid Dynamics Laboratory coupled general circulation model forced with varying concentrations of greenhouse gases.

The dominant modes of SLP both represent much of the total variability and remain important in warmer climates. With SAT, however, the dominant modes are often related to variations in the sea-ice edge and so do not remain important once the ice has retreated; those unrelated to sea ice remain dominant in the warmer climates but represent smaller fractions of the total variability.

In general, climate change tends to project most strongly onto the more dominant modes. The change in SLP projects partially onto the top two modes in the Northern Hemisphere, reflecting both an overall decrease in hemispheric SLP as well as the pattern of change. In the Southern Hemisphere the change projects negligibly onto the dominant patterns between equilibrium climates but very strongly onto the Antarctic oscillation–like mode in the transient integrations. Changes in SAT project partially onto the dominant modes but relate more to the mean warming rather than the pattern of change. In general, the change projects most strongly onto the more dominant modes.

In all SLP domains, the projection of climate change overwhelmingly manifests itself as a linear translation in the mode, consistent with the linear interpretation. In SAT domains related to sea-ice variability, the projection reflects an increased tendency toward ice-free regimes, consistent with the nonlinear perspective; however this nonlinear projection represents only a small portion of the overall climate change.

1. Introduction

A basic issue in climate studies is the nature of the response of the climate system to the enhanced radiative forcing produced by increasing atmospheric concentrations of greenhouse gases. Recently there has been considerable interest in the possibility that this change may project directly onto the preexisting natural modes of variability of the climate system. However, this projection could take one of several different forms, depending, for instance, upon whether the dynamics of the change are linear or nonlinear. The climate change could also project onto several modes or alternatively just a single pattern of variability. Knowledge of the existence and nature of such projections would greatly enhance our ability to both detect and project climate change. In an attempt to expand this knowledge, this paper consists of a simple evaluation of two interpretations of this projection based on linear and nonlinear perspectives of the climate system, using integrations of a coupled general circulation model (GCM).

Support for hypotheses of the projection of enhanced greenhouse warming onto the dominant modes comes from analyses of both the observational record and GCM output. For example, evidence of recent trends in the Arctic oscillation (AO; Thompson and Wallace 1998, 2000) and the Antarctic oscillation (AAO; Rogers and van Loon 1982; Thompson and Wallace 2000) suggest that they represent substantial fractions of the change in the respective hemispheric climate (Thompson and Wallace 2000). In transient integrations of their respective GCMs Fyfe et al. (1999) and Shindell et al. (1999) both noted trends in the mode of sea level pressure (SLP) representing the AO, corresponding in sign to the observed trend. Fyfe et al. (1999) and Kushner et al. (2001) also observed similar trends in the simu-

Corresponding author address: Dáithí A. Stone, School of Earth and Ocean Sciences, University of Victoria, P.O. Box 3055, Victoria, BC V8W 3P6, Canada.
E-mail: stone@ocean.seos.uvic.ca

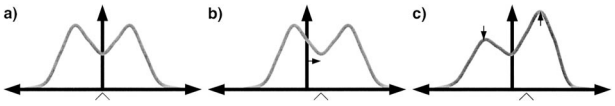

FIG. 1. Comparison of linear and nonlinear interpretations of the projection of climate change. Suppose a hypothetical mode of climate variability has the multimodal PDF shown in (a). Climate change could project (b) linearly onto this mode through a translation of the PDF, or (c) nonlinearly through a change in the shape of the PDF, in this case a shift in the residence frequency of the two regimes associated with this mode. Note that both types of projection result in shifts in the mean of the PDF, indicated by the chevron.

lated AAO, and found that these trends in fact represented almost the entire Southern Hemisphere SLP response.

In interpreting these projections of climate change onto the dominant modes of variability, the simplest case views the climate system from a linear perspective. In this interpretation, the climate change manifests itself through a translation of the mean state of the mode (Fig. 1). For example, a linear translation in the AAO could result from a linear change in the Antarctic Ocean–Antarctica temperature gradient. Support for this interpretation comes from the analyses of monthly GCM output of Fyfe et al. (1999) and Shindell et al. (1999), which suggest translations of Gaussian variables.

On the other hand, a nonlinear perspective of the climate system can lead to a different interpretation of the projection. Palmer (1999) considered the case of a weak forcing on a simple nonlinear system as an analogy to enhanced greenhouse forcing on the climate system, and suggested that the resulting climate change would be reflected in a shift of the residence frequency of the system in certain quasi-stationary regimes. This shift would be visible as a change in the shape of the probability density function (PDF) of the principal components (PCs) associated with these regimes (Fig. 1). However, as a consequence of the stability of the climate attractor, the location and physical structure of these regimes would remain constant, and thus the structure of the corresponding empirical orthogonal functions (EOFs) would remain relatively unaffected.

Corti et al. (1999) examined this interpretation in the Northern Hemisphere mean monthly extended winter 500-hPa geopotential height from reanalysis output, covering the latter half of the twentieth century. They detected multimodality in the system, although Hsu and Zwiers (2000) found that only one of the regimes, corresponding to the so-called ''cold ocean and warm land'' pattern (Wallace et al. 1996), is robust. Noting changes in the structure of this multimodality over time, Corti et al. (1999) suggested that climate change experienced over this period was reflected in a shift in the residence frequency of the climate system in these regimes.

HsZw also analyzed the 500-hPa geopotential height field, but from equilibrium integrations of a coupled GCM, and found that while the locations of the robust regimes were insensitive to the greenhouse forcing, the occupation statistics changed, consistent with the nonlinear interpretation. Monahan et al. (2000a) also examined extratropical Northern Hemisphere SLP from these same equilibrium integrations using a nonlinear PC analysis and found substantial changes in the occupation statistics of the leading nonlinear PC in a warmer climate. Furthermore, Monahan et al. (2000b) found that the recent trend in the observed AO is better defined as a change in the occupation statistics of associated quasi-stationary regimes.

In this nonlinear perspective of the atmospheric system, fluctuations between different regions of the atmospheric attractor occur on timescales of around one week. However, such a perspective can be altered to reflect timescales representative of the coupled ocean–atmosphere climate system. Evidence for regimelike behavior on these timescales exists in the form, for example, of the Pacific decadal oscillation (Mantua et al. 1997). Of course, some modes, such as the AO, are predominantly atmospheric in nature and thus likely do not exhibit regime behavior on these interannual timescales.

This paper aims to evaluate both of these linear and nonlinear interpretations of enhanced greenhouse warming projecting onto the dominant modes of variability, on the longer timescales representative of coupled ocean–atmosphere dynamics. We do this by examining the differences between annual mean SLP and surface air temperature (SAT) fields from 1000-yr equilibrium integrations of the Geophysical Fluid Dynamics Laboratory (GFDL) coupled GCM run with different greenhouse gas forcing. These surface fields are used since it is at this level that the principal components of the climate system interact. Of course, real changes in radiative forcing occur gradually, and so conclusions derived from these equilibrium fields are further tested on the same fields from two transient integrations of the same GCM.

The outline of the rest of this paper is as follows. Section 2 consists of a brief description of the GFDL coupled model and the output fields, and section 3 contains a brief outline of the methods used to analyze the variability of these fields. The nature of the dominant modes of variability is examined in section 4. Since the linear interpretation being considered depends upon the physical structure of these modes remaining invariant in warmer climates, the stability of the modes between different climates is also tested. In section 5 we study the spatial projection of the mean changes in the output fields under different greenhouse gas forcing onto the dominant modes of variability, thus testing whether the climate change projects onto the dominant modes. We then examine the PDFs of the climate system in the space spanned by the corresponding PCs in section 6 in order to differentiate between the linear and nonlinear interpretations. Section 7 consists of a discussion of the results from the previous sections.

2. The GFDL model output

We give only a brief description of the GFDL coupled model; for more details see Manabe et al. (1991) and Stouffer and Manabe (1999). It consists of general circulation models of the atmosphere and ocean, as well as land surface and sea-ice models. Its domain is global and its geography is realistic within the limits of the resolution.

The atmospheric component has nine vertical finite difference levels with horizontal distributions of atmospheric variables represented by spherical harmonics (15 Legendre functions associated with 15 Fourier components) and by gridpoint values (Gordon and Stern 1982). Insolation varies seasonally but not diurnally. Cloud cover is predicted based on relative humidity, while a simple land surface model is used to compute surface fluxes of heat and water (Manabe 1969).

The oceanic component (Bryan and Lewis 1979) employs a full finite-difference technique and uses a regular grid system with approximately 4.5° latitude by 3.7° longitude spacing. There are 12 vertical levels in the ocean. A simple sea-ice model is also included that computes sea-ice thickness based on thermodynamic heat balance and advection of sea ice by ocean currents. The atmospheric, oceanic, and sea-ice components exchange fluxes of heat, water, and momentum once per day.

The coupled model's quasi-equilibrium initial condition is obtained by separate integrations of the atmospheric and oceanic components using the observed surface boundary conditions. When the integration begins from this initial state, the model drifts toward its own less realistic state. To prevent this drift, the fluxes of heat and water are modified by flux adjustments. These adjustments are determined prior to the coupled integration and do not change through the course of the integration; thus they neither systematically damp nor amplify the surface anomalies that occur during the course of the integration. Although the adjustments do not eliminate the shortcomings of the model (Marotzke and Stone 1995), they do help prevent the rapid drift of the model from its initial state.

Three multiple-millennia integrations have been carried out using this coupled model. In the first, the control integration, no changes were made to the radiative forcing in the model. In the other two integrations, the CO_2 concentration in the model's atmosphere increased at a rate of 1% yr^{-1} to doubling ($2 \times CO_2$) and quadrupling ($4 \times CO_2$). These two increased-CO_2 integrations were then run to equilibrium with the radiative forcing held constant at $2\times$ and $4 \times CO_2$, respectively. In this model, it takes about 4000 yr to reach a statistical equilibrium.

For the analysis shown here, the annual mean SAT and SLP fields from 1000-yr segments are used from all three integrations. The use of 1000-yr time series allows very accurate sampling of variability on timescales shorter than 100 yr. Output from two transient integrations of this model, with CO_2 level rising at 1% yr^{-1} from $1\times$ to $2\times$ (70 yr) and from $1\times$ to $4\times$ present levels (140 yr), is also examined to confirm the results in changing climates.

3. Method

The climate modes examined in this analysis are defined as the top EOFs of the output fields, using extratropical hemispheric (poleward of 20° lat) or global domains where appropriate. EOFs in the control integration are retained provided they are clearly separated according to the criterion of North et al. (1982). If ''real'' dynamical modes are important contributors to global variability, higher-order EOFs will represent the same variability, albeit perhaps via linear combinations rather than individual patterns. Furthermore, there is no a priori reason to suppose that climate change will project onto the top mode and not the lesser ones. Therefore, higher-order EOFs are retained, with the understanding that projection of climate change onto the dominant modes may be detected without the possibility of identifying the exact mode.

In standard PC analysis areas with larger variance, for instance SAT at the sea-ice edge, tend to dominate the EOFs. This drowns out patterns of variability in areas with smaller variance that may nevertheless be important for global climate. A solution is to standardize the data fields before conducting the PC analysis. In this study we examine the EOFs of both the output fields and their standardized versions, hereinafter referred to as the physical output fields and the standardized output fields, respectively. The physical EOFs tend to focus on higher latitudes, since the variance in SLP and SAT is largest there; the lower-latitude variability is relatively more important in the standardized EOFs.

To examine the possible importance of regime behavior, we examine the SLP and SAT fields in a reduced space in the same manner as Kimoto and Ghil (1993), Brunet (1994), Corti et al. (1999), and HsZw (see section 6). The two-dimensional PDFs in the space spanned by the leading two PCs are estimated using an adaptive kernel estimator (Silverman 1986; Kimoto and Ghil 1993). This nonparametric method uses all of the values in the PCs, weighted according to a kernel function (here the Gaussian kernel), to estimate the value of the PDF at each point. The optimal smoothing parameter, h, of this estimator, which determines the effective radius of influence of the kernel function, is determined as the location of the minimum of a score function $m(h)$.

4. The dominant modes of variability

In order for the linear interpretation of climate change projecting onto the dominant modes of variability to be viable, these modes must remain important in the warmer climates. However, this requirement may not always hold in the nonlinear interpretation evaluated here, since if the climate system tends toward residing overwhelm-

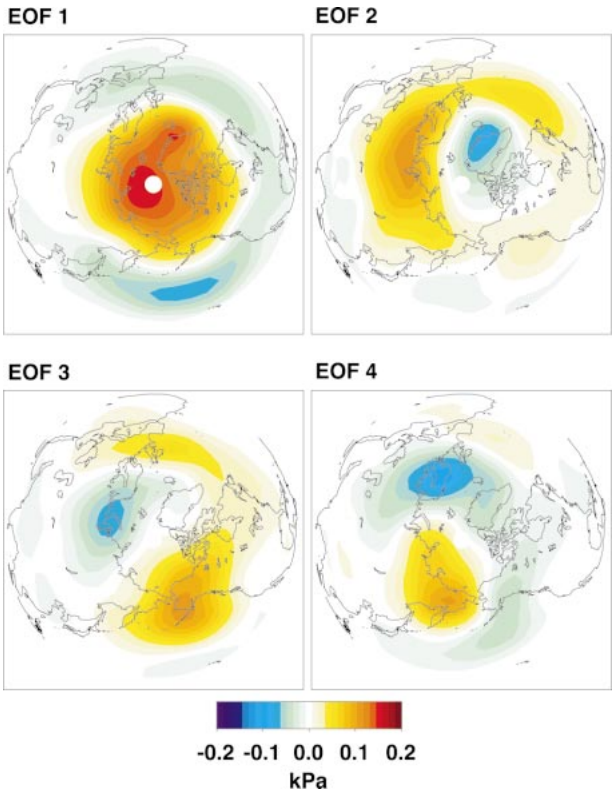

FIG. 2. The top four EOFs of extratropical Northern Hemisphere physical SLP in the control integration.

ingly in only one regime, fluctuations between this regime and others will occur less frequently and thus the mode of variability associated with these fluctuations will be less important. This section presents the dominant modes of variability of the SLP and SAT fields extracted using PC analysis and examines whether they remain important in climates with higher greenhouse gas concentrations.

The EOFs of physical SLP are presented first in the domain of extratropical hemispheres; those in the global domain closely resemble their hemispheric counterparts and so are ignored in this analysis. The subsequent section examines the EOFs of standardized SLP over the global domain, which brings out patterns in the Tropics, unlike the EOFs of physical SLP. Because of this importance of the Tropics, the standardized SLP cannot be examined in the hemispheric domains. This ordering is then repeated for the EOFs of SAT.

a. Extratropical Northern Hemisphere physical SLP

The top four EOFs of extratropical Northern Hemisphere SLP (Fig. 2) all satisfy the criterion of North et al. (1982). The first EOF, resembling the AO (Thompson and Wallace 1998; 2000), and EOFs 2 and 3 are quite similar to the top three EOFs of extended winter monthly mean SLP found by Fyfe et al. (1999) in a control integration of the Canadian Centre for Climate Modelling and Analysis (CCCma) GCM and in the observational record. The main differences in our EOFs are the strong variability in the North Pacific, as noted by Hall and Visbeck (2000, manuscript submitted to *J. Climate*), and the importance of the Eurasian center in EOFs 2 and 3. In the control integration these patterns represent 23%, 9%, 8%, and 6% of the variance, respectively. The first EOF remains practically unchanged in the warmer climates, while the second and third EOFs appear to mix in the warmer climates but nevertheless remain important. The intensities of the centers in the fourth EOF vary in the warmer climates, but the basic tripole pattern remains.

b. Extratropical Southern Hemisphere physical SLP

The first EOF of extratropical Southern Hemisphere SLP (Fig. 3) resembles the AAO (Rogers and van Loon 1982; Thompson and Wallace 2000), while the second EOF (Fig. 3) resembles an average of the second EOFs of SLP found in the observational record by Rogers and

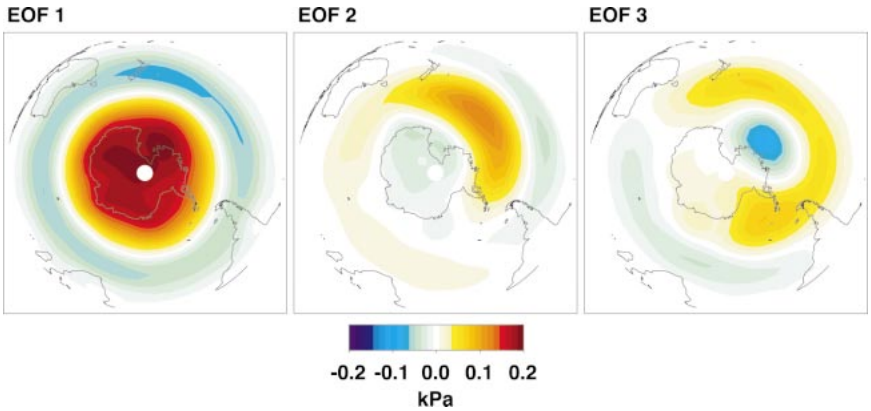

FIG. 3. The top three EOFs of extratropical Southern Hemisphere physical SLP in the control integration.

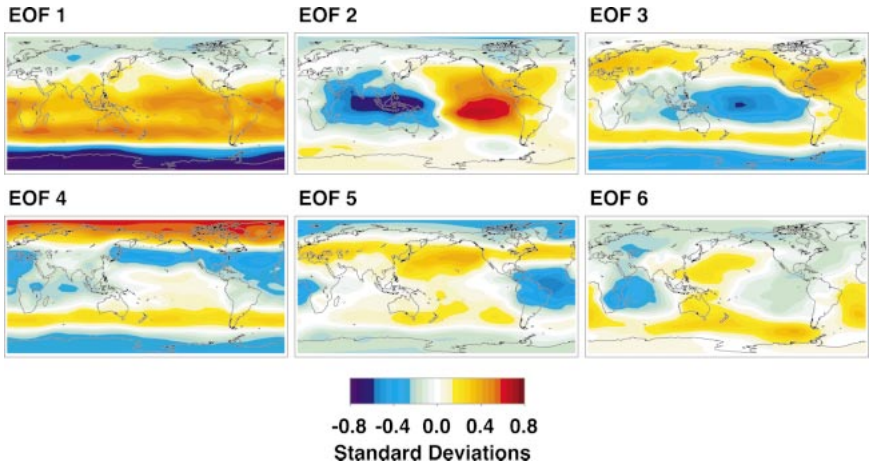

FIG. 4. The top six EOFs of global standardized SLP in the control integration.

van Loon (1982) in the winter and summer seasons. The top three EOFs represent 41%, 7%, and 5% of the variance in the control integration, respectively. The first EOF remains practically unchanged in the warmer climates, while the center in the second EOF weakens and shifts westward in the warmer climates, but continues to remain important. The third EOF, however, is not retrieved by PC analysis of the warmer climate fields, although the pattern still accounts for an important portion of the variability in these climates.

c. Global standardized SLP

The first six EOFs (Fig. 4) of global standardized SLP all satisfy the criteria outlined above. The first and fourth EOFs are similar to the AAO and AO, respectively, but the midlatitude band extends over the Tropics in both cases, reflecting the stronger role of this region in this standardized domain. The importance of the Tropics is further illustrated in the second EOF, which resembles the Southern Oscillation. Of particular note, the first EOF appears to partially represent a Tropics-to-poles mode of variability along with the AAO. This dual representation implies that neither mode is fully represented, resulting in ''echoes'' of this structure in EOFs 3, 4, and 5. These six patterns represent 12%, 9%, 6%, 5%, 4%, and 3% of the standardized variance, respectively. All of the patterns retain their overall structure in the warmer climates, with the largest differences related to the magnitude of the Tropics-to-poles structure.

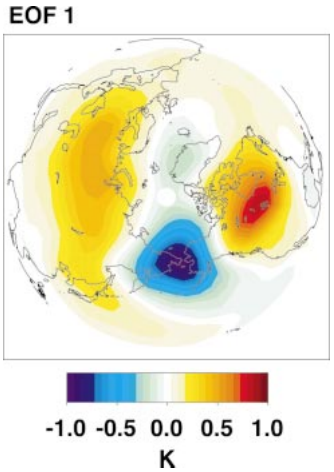

FIG. 5. The top EOF of extratropical Northern Hemisphere physical SAT in the control integration.

d. Extratropical Northern Hemisphere physical SAT

Only the first EOF of extratropical Northern Hemisphere physical SAT (Fig. 5), representing 10% of the variance in the control integration, clearly satisfies the criterion of North et al. (1982). Because of the relatively small variance of SAT in the Tropics, this EOF closely resembles the top EOF of SAT north of 50°S found by Barnett (1999) in a separate 1000-yr segment of the same multiple-millennia integration used here. The Eurasian center shifts eastward in the warmer climates, but the main tripole pattern is maintained.

e. Extratropical Southern Hemisphere physical SAT

The largest variations in physical SAT in the extratropical Southern Hemisphere occur around Antarctica, and consequently the top EOFs are concentrated in this region (Fig. 6). The PCs associated with the top two EOFs clearly represent fluctuations between ice-covered and ice-free regimes. The top three EOFs represent 27%, 14% , and 6% of the variance in the control integration. Since these patterns are related to changes in sea-ice extent, they do not remain important in the warmer climates, when the ice has retreated. Thus, only the nonlinear interpretation of climate change projection can be examined in this domain in later sections.

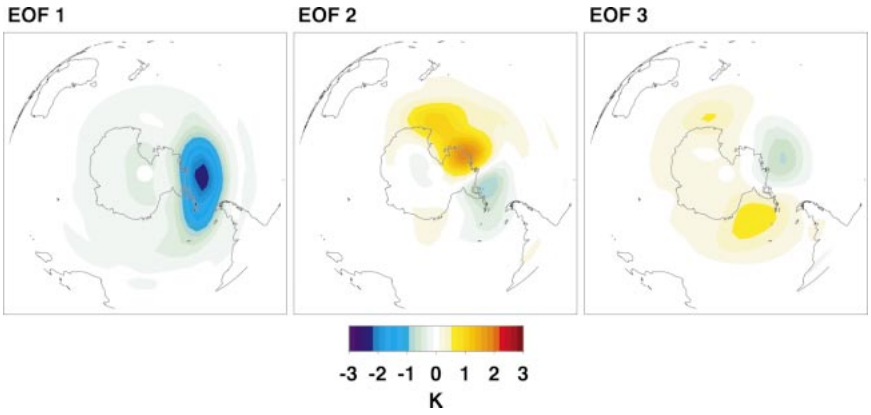

FIG. 6. The top three EOFs of extratropical Southern Hemisphere physical SAT in the control integration.

f. Global standardized SAT

The top three EOFs of global standardized SAT (Fig. 7) all satisfy the separation criterion of North et al. (1982). The first EOF represents an El Niño/La Niña–like warming and cooling in the tropical Pacific Ocean. At least partly due to the coarse ocean resolution, the El Niño–Southern Oscillation (ENSO) simulated by the GFDL model is weaker than the observed (Knutson and Manabe 1994), and so this pattern is not detected in physical SAT. The second EOF resembles the first EOF of Southern Hemisphere physical SAT, while the third pattern bears a close resemblance to the top EOF of extratropical Northern Hemisphere physical SAT. These three patterns represent 7%, 4%, and 3% of the variance of global standardized SAT in the control integration respectively. Since it represents sea-ice variability, the second EOF weakens as the sea ice retreats, and so only the first and third EOFs remain important in the warmer climates. Knutson and Manabe (1994) also noted that ENSO variability, represented here by the first EOF, does not change in the warmer climates.

The top EOFs of SLP account for an important fraction (40%–50%) of the variability in all domains. They also generally remain important in the warmer climates, with only relatively small changes occurring in their structure. On the other hand, many of the top EOFs of SAT represent variations in sea-ice extent; with the retreat of the sea-ice edge these modes cease to remain important in the warmer climates. However, the top SAT EOFs unrelated to sea-ice variability do remain important in the warmer climates. Nevertheless, they account for a smaller portion (~10%) of the variability. Since they remain important in the warmer climates, SAT patterns unrelated to sea-ice variability, as well as SLP patterns, may be consistent with the linear or nonlinear interpretations of climate change projecting onto the dominant modes of variability. On the other hand, those SAT patterns associated with sea-ice variability, which changes considerably in the warmer climates, may be consistent with only the nonlinear interpretation.

5. Spatial projection of climate change

Because EOFs represent the preferred direction of variability of the climate system, forced climate change may project directly onto these modes. In this section we test this possibility by examining the spatial projection of the climate change onto these patterns. We do this by taking the mean difference between the 2× and 4 × CO_2 equilibrium integrations and the control integration and then projecting these fields onto the top EOFs of the control integration. Of course, the actual rise in greenhouse gas concentrations is occurring gradually; thus the patterns of the mean trends in the output

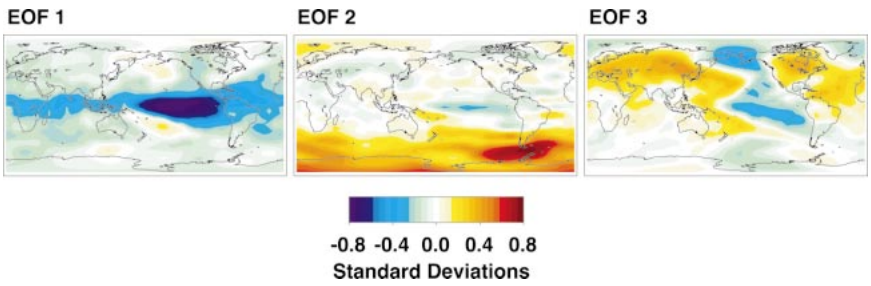

FIG. 7. The top three EOFs of standardized global SAT in the control integration.

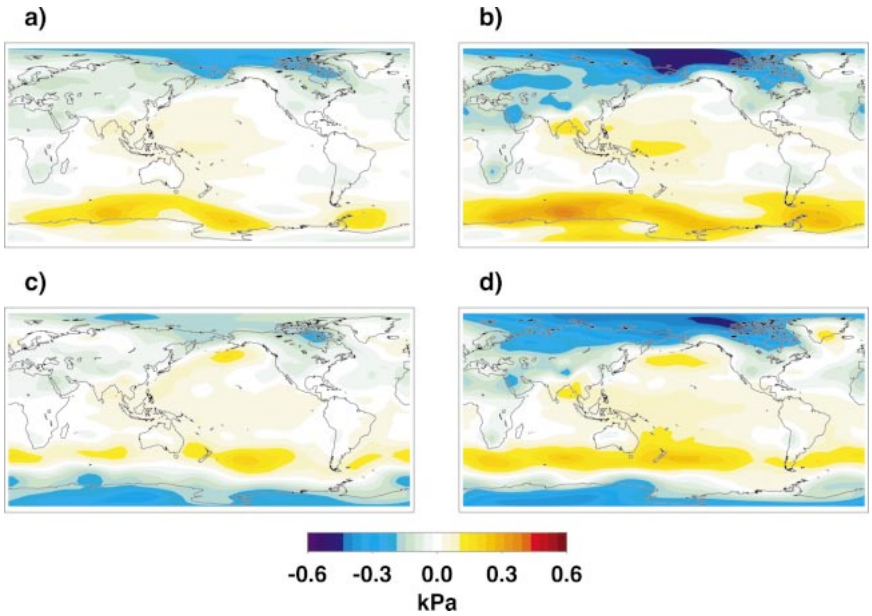

FIG. 8. The change in physical SLP occurring under enhanced greenhouse forcing. The mean difference between the (a) 2 × CO_2 and (b) 4 × CO_2 equilibrium integrations and the 1 × CO_2 control integration is shown, along with the total trend in the (c) 1–2 × CO_2 and (d) 1–4 × CO_2 transient integrations.

of the two transient integrations are also projected onto the control EOFs to confirm or differentiate the results in changing climates. A point to note is that both the difference fields and the EOFs often have nonzero means, since they are either defined in hemispheric domains or they are not constrained globally. This implies that the projection reflects both similarities in the pattern and in the direction of the change.

a. Extratropical Northern Hemisphere physical SLP

The mean changes in physical SLP under enhanced greenhouse forcing are displayed in Fig. 8. A notable feature of these changes in the Northern Hemisphere is their structural similarity, reflecting a fairly linear, and seemingly robust, change in global mean SLP in the warmer climates. The projection of these difference fields onto the top EOFs of physical SLP is plotted in Fig. 9. It must be reminded that these projections reflect both the pattern and direction of the change. Roughly one-third of the change projects onto the AO-like mode. Fyfe et al. (1999) noted a similar projection onto the top EOF of wintertime monthly mean SLP in the Northern Hemisphere in a transient integration of the CCCma coupled model, although they also found a comparable

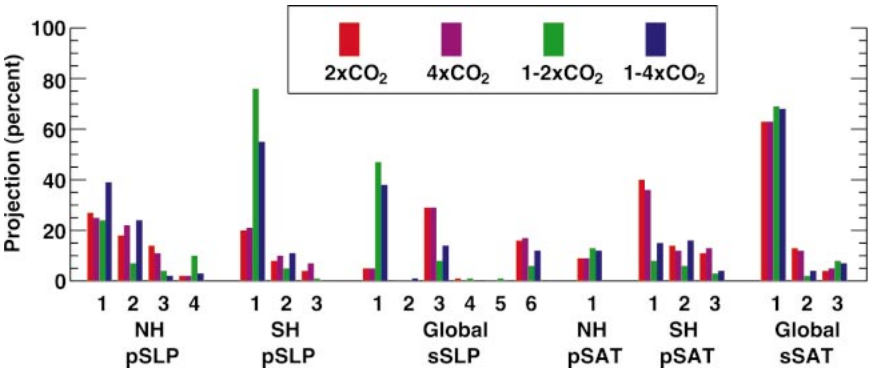

FIG. 9. The spatial projection of enhanced greenhouse-forced climate change onto the top EOFs of the control integration. Both the difference fields and EOFs often have nonzero means, so the projection reflects both the pattern and direction of the change. The EOFs in each domain are labeled by their rank (1 through up to 6); see Figs. 2–7 for depictions of each EOF (NH = Northern Hemisphere; SH = Southern Hemisphere; pSLP = physical SLP; sSLP = standardized SLP; pSAT = physical SAT; sSAT = standardized SAT).

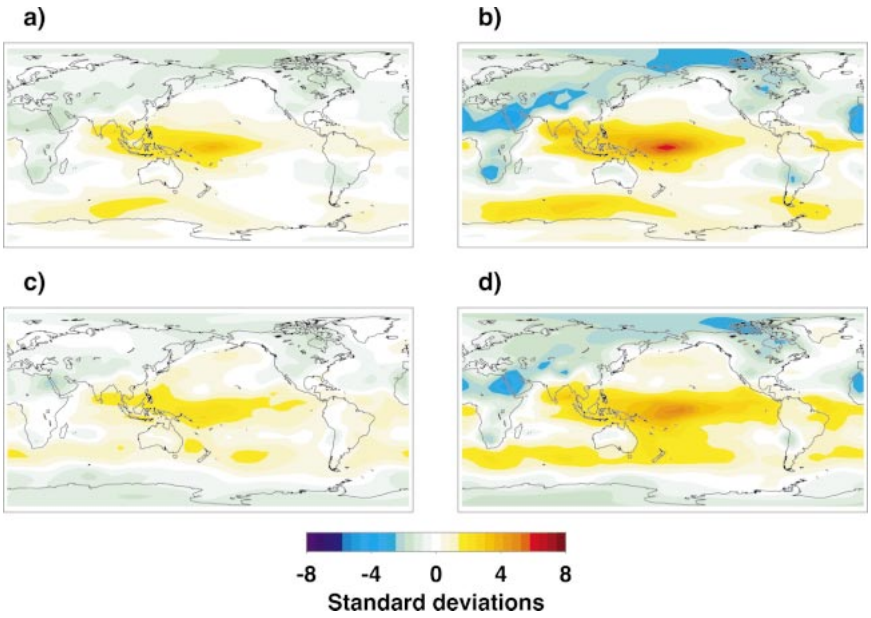

FIG. 10. As in Fig. 8 but for standardized SLP.

projection onto their third EOF. Instead, we see a similar projection onto the second EOF, which is actually related more to the general decrease in pressure in the Northern Hemisphere than to the pattern of the change.

b. Extratropical Southern Hemisphere physical SLP

In the Southern Hemisphere the mean change in physical SLP between the equilibrium integrations (Fig. 8) projects only partially onto the top modes (Fig. 9). However, the mean trends in the two transient integrations differ substantially, projecting quite strongly onto the AAO-like mode. This difference likely results from the delay of the sea-ice retreat and ocean warming in the Antarctic Ocean in the transient integrations. These results bear a striking resemblance to those of Fyfe et al. (1999) who found that in their transient integration of a coupled GCM the change in the Southern Hemisphere projected almost entirely onto the AAO-like pattern. Kushner et al. (2001) also observed this projection onto the AAO in the output of a higher-resolution version of the GFDL coupled GCM than that used here. The implication of the difference between the equilibrium and transient changes here is that this is purely the initial response to climate change, with the AAO reverting to its original state once the climate system has evolved further.

c. Global standardized SLP

As with physical SLP, the changes in standardized SLP (Fig. 10) are structurally similar for the 2× and 4 × CO_2 climates. However, the differences are not confined to the high latitudes, instead reflecting a land–ocean difference. This change projects partly onto the third EOF (tropical Pacific–North Atlantic dipole), and negligibly onto the other modes (Fig. 9). As with physical SLP, the changes in the transient integrations differ from that between the equilibrium integrations in the Southern Hemisphere, with the trend projecting fairly strongly onto the AAO-like mode, represented by the first EOF.

d. Extratropical Northern Hemisphere physical SAT

As with SLP, the spatial structure of the change in physical SAT in the Northern Hemisphere (Fig. 11) is similar in all integrations. It is also concentrated in high latitudes, due to the large ice albedo feedback. Nevertheless, this pattern projects negligibly onto the top EOF of this domain (Fig. 9).

e. Extratropical Southern Hemisphere physical SAT

In the Southern Hemisphere about 40% of the change in physical SAT between the equilibrium integrations (Fig. 11) projects onto the first EOF (Fig. 9). This is related both to the pattern and direction of the change, although it does not account for the largest warming, which occurs in the Ross Sea. Because of the lag in the ocean warming and sea-ice retreat in the transient integrations, the mean trends are much smaller than the equilibrium changes. The differences in the spatial pattern of warming between the two transient integrations

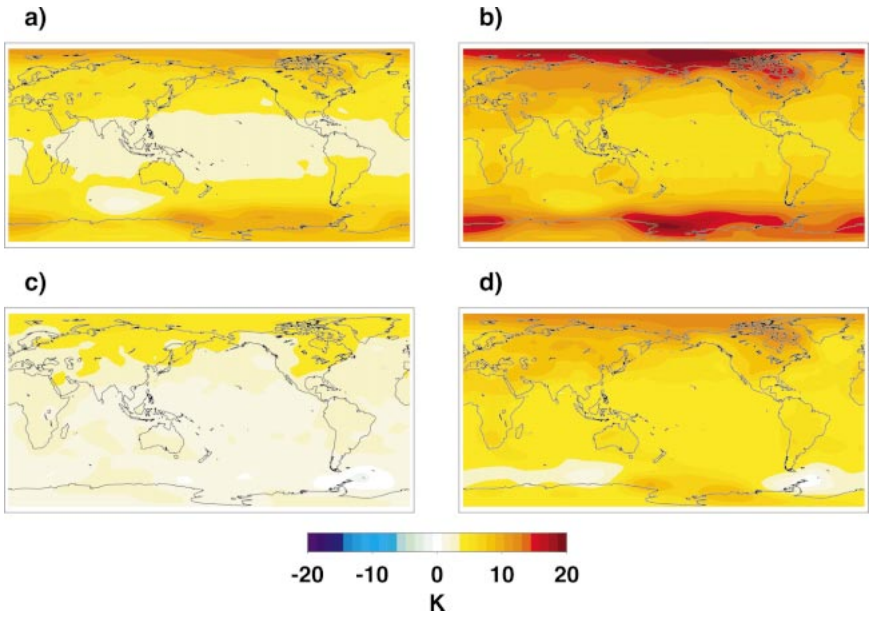

FIG. 11. As in Fig. 8 but for physical SAT.

suggests that the location of the initial ice retreat in the Antarctic may be somewhat random.

f. Global standardized SAT

The changes in standardized SAT (Fig. 12) are structurally quite similar for the 2× and 4 × CO_2 climates, with the largest differences over the Tropics, but they differ from the trends in the transient integrations in high southern latitudes. In all integrations the change projects fairly strongly onto the ENSO-like mode (Fig. 9); however, this is strongly reflective of the general warming. Furthermore, the pattern of change itself reflects simply a difference between the tropical and high latitudes and does not resemble the ENSO pattern at smaller scales, and thus a projection onto the ENSO-like mode would appear to be largely spurious.

The analysis of Northern Hemisphere physical SLP supports the results of Fyfe et al. (1999) that climate change will project only weakly onto the dominant modes in the Northern Hemisphere. Furthermore, the strong projection of climate change onto the AAO-like

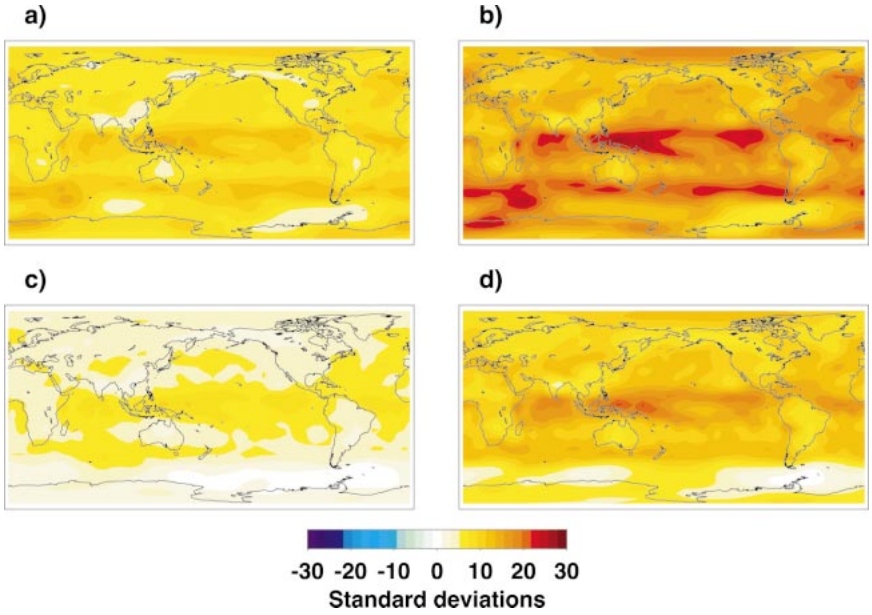

FIG. 12. As in Fig. 8 but for standardized SAT.

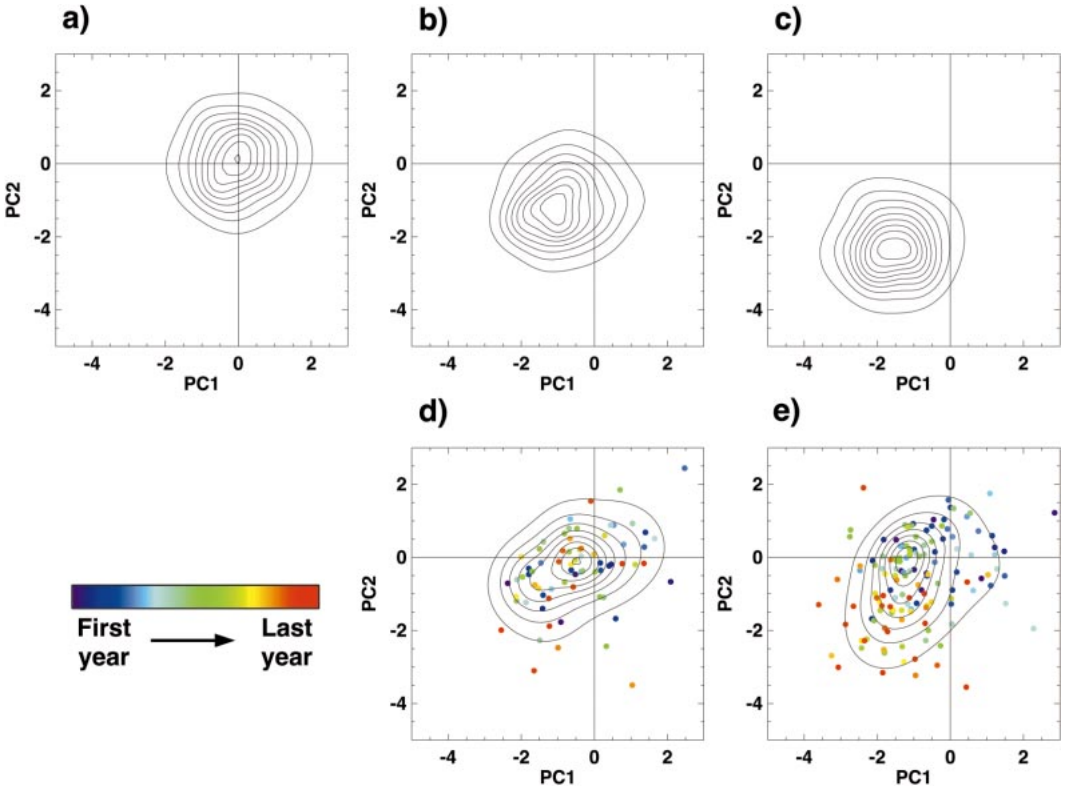

FIG. 13. The estimated PDFs of physical SLP in the space spanned by the top two PCs of the 1 × CO_2 control integration in the extratropical Northern Hemisphere. The PDFs from (a) a second 1 × CO_2, (b) the 2 × CO_2, and (c) the 4 × CO_2 equilibrium integrations, and the (d) 1–2 × CO_2, and (e) 1–4 × CO_2 transient integrations are shown. See section 3 of the text for a description of the generation of these estimated PDFs. For (a), (b), and (c) a smoothing parameter of $h = 0.4$ is used, and for (d) and (e) a value of $h = 0.675$ is used. Contours denote multiples of 0.02, and the units on the axes are the std dev of the PCs in the control integration. In (d) and (e) the colored dots represent each annual mean realization of the climate system in this reduced space.

mode in the Southern Hemisphere found by Fyfe et al. (1999) and Kushner et al. (2001) is reproduced here in the transient integrations. However, the negligible projection between equilibrium integrations suggests that this constitutes only the initial, purely atmospheric response, and disappears once the sea ice has retreated and the ocean has warmed. The projection of the enhanced greenhouse-forced change in SAT onto the SAT modes is generally more representative of the overall warming rather than the spatial pattern of that warming. Inspection of Fig. 9 shows that the change tends to project most strongly onto the more dominant modes. While this may be related in part to the greater spatial coherence of the more important EOFs, it nevertheless suggests that climate change will indeed tend to project onto the more dominant modes. Only in one case does this actually constitute most of the response, but it would be naive to assume that the simple implementation of linear PC analysis of annual mean output used here has extracted all of the important modes in the climate system.

6. The nature of the spatial projection

The results of section 5 demonstrate that forced climate change can project onto some of the dominant modes of variability. However, they do not differentiate between whether that projection is linear or nonlinear, that is whether the projection reflects a linear translation in the climate system or a shift in the residence frequency of the system in regimes associated with these modes. This section aims to distinguish between these two possibilities by examining the PDFs of the climate system in reduced spaces spanned by the top PCs of the control integration.

a. Extratropical Northern Hemisphere physical SLP

The estimated PDFs of physical SLP in the space spanned by the top two PCs of the control integration in the extratropical Northern Hemisphere are plotted in Fig. 13. This space represents about one-third of the variance in the control integration, while around one-half of the change due to enhanced greenhouse forcing projects onto it. The PDF from the 1 × CO_2 integration (Fig. 13a) resembles a Gaussian distribution centered on the origin. A separate 1000-yr segment of the multiple-millennia 1 × CO_2 integration was used here to reduce the bias when projecting onto the EOFs of the

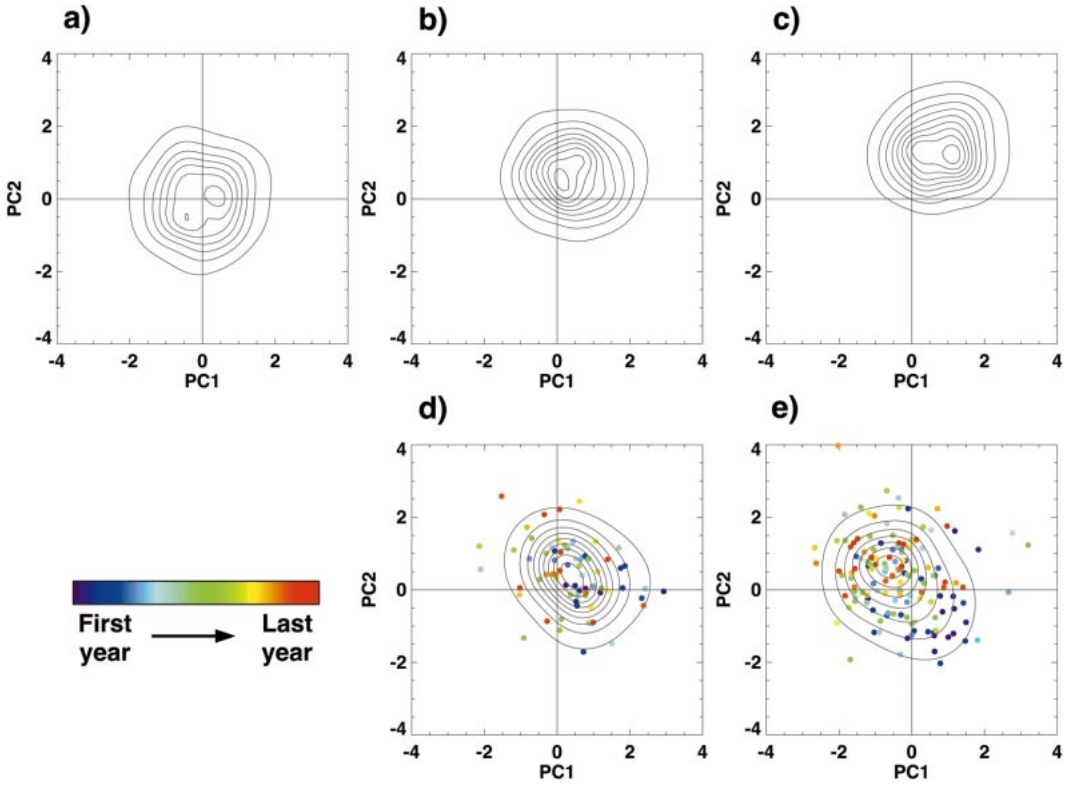

FIG. 14. As in Fig. 13, but for the estimated PDFs of physical SLP in the space spanned by the top two PCs of the control integration in the extratropical Southern Hemisphere.

control segment of the integration. There is no clear evidence of multimodality, suggesting that these modes are not related to fluctuations between regimes on the timescales examined here.

The changes in the warmer climates (Figs. 13b and 13c) are dominated by a translation of the PDF, with no obvious changes occurring in its shape. The PDFs from the transient integrations (Figs. 13d and 13e) indicate that this translation is linear. Consistent with this, the annual mean state, represented in Fig. 13 by the colored dots, progresses gradually from the $1 \times CO_2$ state to the warmer states. Thus, in the Northern Hemisphere the projection of change in physical SLP appears overwhelmingly linear on interannual timescales.

b. Extratropical Southern Hemisphere physical SLP

The estimated PDFs of physical SLP in the extratropical Southern Hemisphere, in the space spanned by the top two PCs of the control integration, are plotted in Fig. 14. As in the Northern Hemisphere, the climate system is relatively Gaussian in this reduced space, and the equilibrium climate change takes the form of a linear migration of the PDF. However, because of the lag in ocean warming and sea-ice retreat, the trends in the transient integrations do not resemble the equilibrium changes, instead reflecting decreasing pressure over Antarctica. The projection onto the AAO-like mode in the transient integrations mimics the projection onto the AO-like mode in the Northern Hemisphere, indicating that this decrease in the gradient between polar and midlatitudes is an atmospheric response.

c. Global standardized SLP

With global standardized SLP, the climate change projects partially onto the first and third EOFs and negligibly onto the remaining top patterns (Fig. 9). The estimated PDFs of standardized SLP in the space spanned by the two corresponding PCs of the control integration are plotted in Fig. 15. As with physical SLP, at $1 \times CO_2$ the PDF of the climate system is relatively Gaussian, and changes occur primarily through a translation in the warmer climates. The change is relatively linear in the transient integrations, progressing gradually from the $1 \times CO_2$ state to the warmer states. This latter point is curious considering that the first EOF represents an AAO-like mode of variability. The representation of this mode in physical SLP in the extratropical Southern Hemisphere (the first EOF) evolves differently in the transient integrations than between the equilibrium integrations. This difference between the standardized and physical versions of this mode must result from the importance of tropical variability in the standardized version.

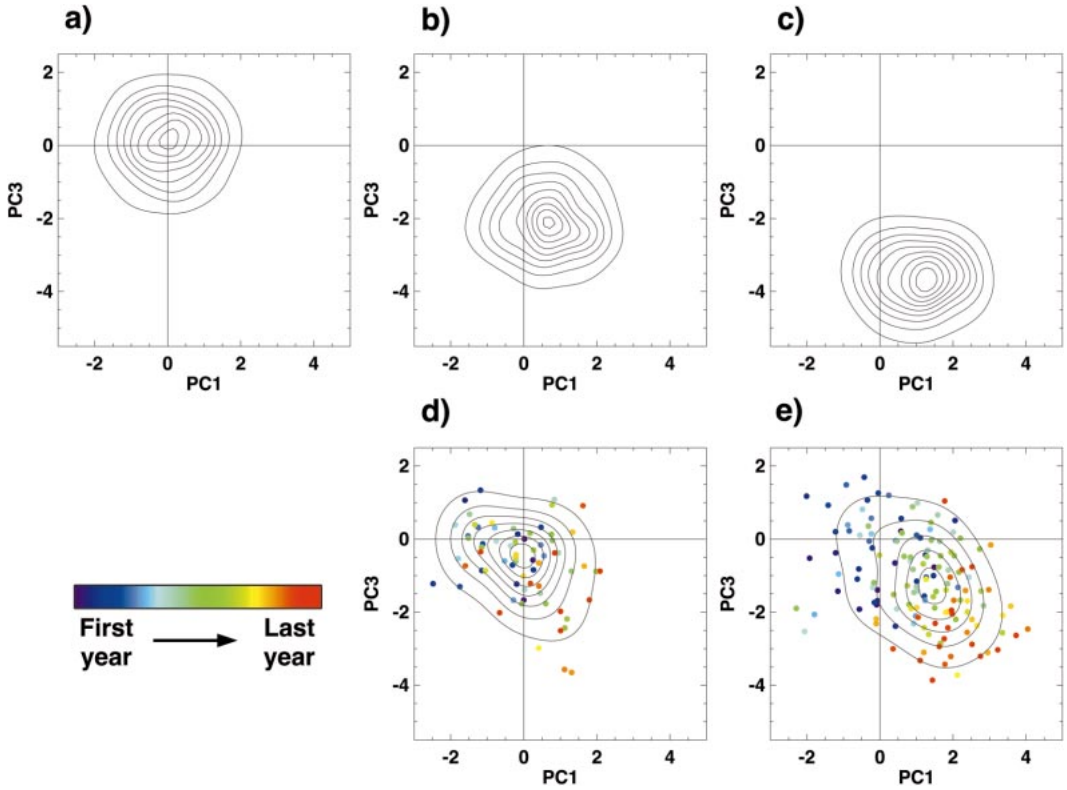

FIG. 15. As in Fig. 13, but for the estimated PDFs of standardized SLP in the space spanned by the first and third PCs of the control integration over the entire globe.

d. Extratropical Northern Hemisphere physical SAT

The sole stable EOF of physical SLP in the extratropical Northern Hemisphere accounts for only a negligible portion of the change under enhanced greenhouse forcing. The estimated PDFs in the space spanned by the corresponding PC of the control integration (not shown) behave similarly to those examined above; the PDFs resemble a Gaussian distribution whose location shifts linearly, but only slightly, as the climate warms.

e. Extratropical Southern Hemisphere physical SAT

The top two PCs of extratropical Southern Hemisphere physical SAT represent fluctuations between ice-free and ice-covered states, resulting in regime behavior clearly visible in Fig. 16. Obviously, in the warmer climates both PCs would tend toward the ice-free regimes. Indeed, the PDF from the $4 \times CO_2$ integration does not reveal any regimelike behavior. Meanwhile, the regime behavior in the $2 \times CO_2$ integration results from sea-ice–related variations very different from that represented by these two EOFs in the $1 \times CO_2$ integrations. Nevertheless, the PCs in the warmer climates have evolved much further than the ice-free regime, reflecting a warming of the ocean. Thus while the climate change does partially project nonlinearly onto the regime behavior of the SAT field here, the linear warming nevertheless dominates. Of course, since these modes do not remain important in the warmer climates, this gradual warming cannot be interpreted using the linear perspective.

f. Global standardized SAT

As with physical SAT in the Southern Hemisphere, the estimated PDFs of global standardized SAT in the space spanned by the top PCs (not shown) indicate some regime behavior. However, once again the linear translation of the climate state dwarfs any changes in the behavior in the modes. Since the first and third EOFs remain important in the warmer climates, this change could be consistent with the linear perspective. However, as noted in section 5, this change primarily reflects the overall warming trend rather than the pattern of that change, and thus the physical reality of this projection is questionable.

The results of section 5 demonstrated that in SLP, substantial fractions of the climate change due to enhanced greenhouse forcing project directly onto the dominant modes of variability. The results of this section indicate that this projection is predominantly linear. Regimelike behavior was generally not evident in the estimated PDFs from the second $1 \times CO_2$ integration, and the climate change largely manifested itself as a

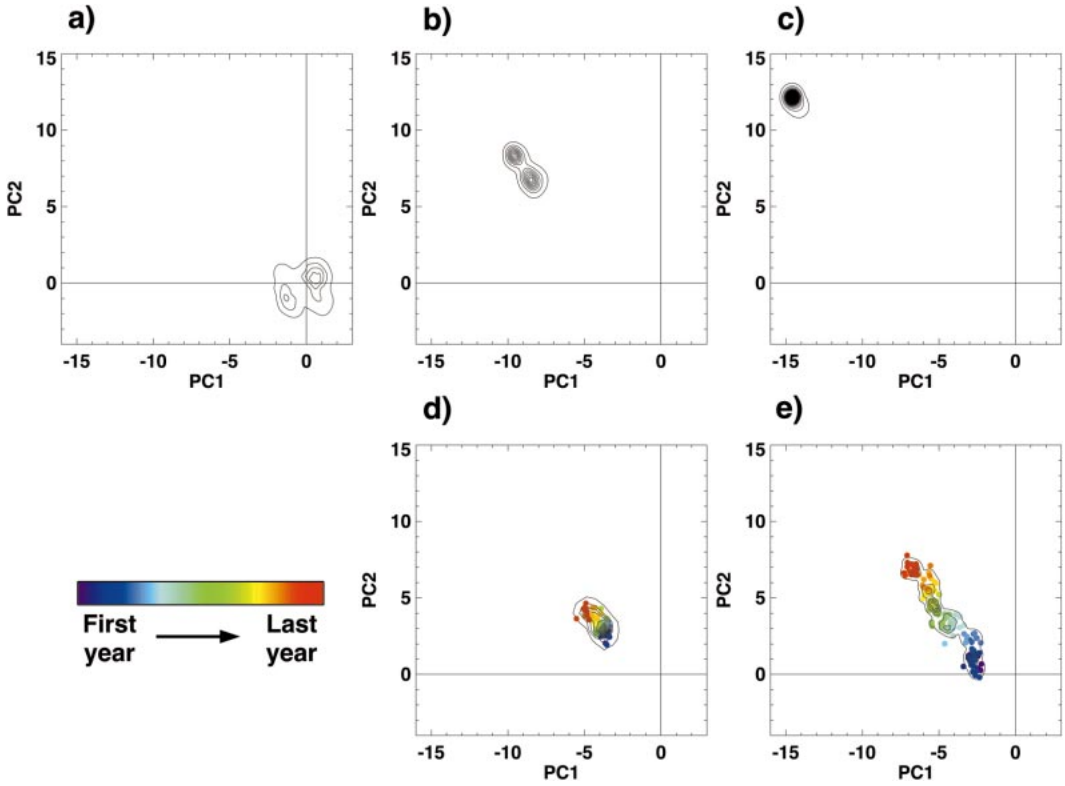

FIG. 16. As in Fig. 13, but for the estimated PDFs of physical SAT in the space spanned by the top two PCs of the control integration over the extratropical Southern Hemisphere. A smoothing parameter of $h = 0.2$ is used. The first contour denotes the 0.02 level, while the other contours represent multiples of 0.08.

linear translation away from the $1 \times CO_2$ state toward states not frequently visited in the $1 \times CO_2$ climate. Unlike SLP, evidence of regime behavior was found for SAT modes related to sea-ice variability. Furthermore, the climate change was partly expressed as a shift of the climate system toward the ice-free regimes.

7. Discussion

Present and future climate change due to increasing anthropogenic emissions of greenhouse gases is now generally accepted (IPCC 2001); however, the nature of that change is still a topic of considerable debate. Here we have evaluated two interpretations of this climate change, whereby it projects onto the preexisting low-frequency natural modes of variability of the climate system, using integrations of a coupled GCM.

In order to interpret the concept of climate change projecting onto the dominant modes of variability, it must be established whether these modes remain important in different climates. It was found that the modes of SLP and those of SAT unrelated to sea-ice variability do indeed remain important. However, modes related to sea-ice variability, which dominate in the Southern Hemisphere, were no longer found to be important in the warmer climates since the sea ice had retreated to different locations. This implies that while the nonlinear perspective of the projection of climate change may apply to all modes, the linear perspective may apply only to the SLP and non–sea-ice SAT modes.

In several of the domains examined, the climate change was found to project directly onto some of the dominant modes of variability. In general, this projection tended to be strongest onto the more dominant patterns. This suggests that the climate change will tend to project onto only a single mode of variability, rather than a combination of the more dominant modes. The change in SAT projected only partially onto the top modes, but this generally reflected the overall warming rather than the pattern of that warming. The changes in SLP, however, tended to represent the pattern of the change, since the mean changes were of much smaller magnitude.

In the Northern Hemisphere, SLP was found to project only partly onto the top two modes. This result, along with the findings of Fyfe et al. (1999), is at odds with the conclusion of Shindell et al. (1999) that a modeled stratosphere is necessary to simulate a trend in the AO, since the GFDL model does not resolve the stratosphere. In the Southern Hemisphere, the change projected almost entirely onto the AAO-like mode in the transient integrations, as was found by Fyfe et al. (1999) and Kushner et al. (2000); however, it projected negligibly between the equilibrium integrations. This sug-

gests that the strong projection onto this pattern is a purely atmospheric response during the period when the climate is changing, while the coupled atmosphere–ocean–sea-ice response is largely unrelated to the AAO. An important question is whether the projection onto the AAO, and the much weaker projection onto the AO, represent only a surface manifestation of a ''monsoon-like'' response, or whether they are effectively barotropic and extend to the higher regions of the annular modes. While this issue was beyond the scope of the present work, the results of Kushner et al. (2001) suggest that indeed this response extends at least up to the tropopause.

In all SLP domains examined, no regime behavior was evident in the projection of the climate state onto the top modes. Furthermore, the climate change manifested itself in a linear translation of these modes, moving far beyond regions of the climate attractor frequented in the control integration. Unlike for SLP, regime behavior was clearly visible in some of the SAT modes, and the residence frequency of the climate system in these regimes did change with enhanced greenhouse forcing. Nevertheless, these changes accounted for little of the projection of the climate change onto these modes, which instead mostly reflected an overall warming, and thus represented only a small fraction of the overall climate change.

An evident caveat to these results is the question of the applicability of the nonlinear interpretation to annual mean fields. In its original formulation by Palmer (1999), this hypothesis interpreted long-term climate change in terms of the high-frequency (~one week) fluctuations of the atmosphere. It should be possible to extend this theory to the lower-frequency interannual variability of the coupled climate system. However, modes operating at higher frequencies than the interannual timescale would not be detected in annual mean data. SLP does not depend as much on oceanic and sea ice variability as does SAT, and notably support for regime behavior was found only in the SAT domain. This implies that the weak support here for the low-frequency nonlinear interpretation does not automatically apply to this interpretation in its original formulation.

This study aimed to test interpretations of climate change projecting onto the dominant modes of variability, based on linear and nonlinear perspectives of the climate system, using integrations of a coupled GCM. Modes of variability of SAT did exhibit behavior consistent with the nonlinear perspective. While changes in SAT did project partially onto these modes, this tended to reflect the overall warming rather than the pattern of the change. Consequently, changes in regime behavior related to the retreat of the sea-ice edge, consistent with the nonlinear interpretation, only represented a small fraction of the climate change. Changes in SLP in the Southern Hemisphere projected very strongly in the transient integrations onto an AAO-like mode in a manner consistent with the linear interpretation; however, this pattern of change was absent between the equilibrium integrations, suggesting that this is purely an atmospheric response. Changes in SLP in other domains only projected partially onto some modes. In general, climate change tended to project most strongly onto the more important modes. These results indicate that climate change may project onto dominant modes of interannual variability in some domains, but not in others, and that this projection will generally be more consistent with the linear perspective on these timescales.

Acknowledgments. The authors wish to thank Gilbert Brunet, Thomas Delworth, John Fyfe, Juno Hsu, Paul Kushner, and Francis Zwiers, as well as Tim Palmer and an anonymous reviewer, for many helpful comments and suggestions. Financial support for this research from the Climate Change Action Fund, the International Arctic Research Centre, the Meteorological Service of Canada/Canadian Institute for Climate Studies, and the National Science and Engineering Research Council is gratefully acknowledged.

REFERENCES

Barnett, T. P., 1999: Comparison of near-surface air temperature variability in 11 coupled global climate models. *J. Climate,* **12,** 511–518.

Brunet, G., 1994: Empirical normal-mode analysis of atmospheric data. *J. Atmos. Sci.,* **51,** 932–952.

Bryan, K., and L. J. Lewis, 1979: A water mass model of the world ocean. *J. Geophys. Res.,* **84,** 2503–2517.

Corti, S., F. Molteni, and T. N. Palmer, 1999: Signature of recent climate change in frequencies of natural atmospheric regimes. *Nature,* **398,** 799–802.

Fyfe, J. C., G. J. Boer, and G. M. Flato, 1999: The Arctic and Antarctic oscillations and their projected changes under global warming. *Geophys. Res. Lett.,* **26,** 1601–1604.

Gordon, C. T., and W. F. Stern, 1982: A description of the GFDL global spectral model. *Mon. Wea. Rev.,* **110,** 625–644.

Hsu, C. J., and F. W. Zwiers, 2000: Climate change in recurrent regimes and modes of Northern Hemisphere atmospheric variability. *J. Geophys. Res.,* in press.

IPCC, 2001: *Climate Change 2001: The Scientific Basis. Contribution of Working Group I to the Third Assessment Report of the Intergovernmental Panel on Climate Change.* Cambridge University Press, in press.

Kimoto, M., and M. Ghil, 1993: Multiple flow regimes in the Northern Hemisphere winter. Part I: Methodology and hemispheric regimes. *J. Atmos. Sci.,* **50,** 2625–2643.

Knutson, T. R., and S. Manabe, 1994: Impact of increased CO_2 on simulated ENSO-like phenomena. *Geophys. Res. Lett.,* **21,** 2295–2298.

Kushner, P. J., I. M. Held, and T. L. Delworth, 2001: Southern Hemisphere atmospheric circulation response to global warming. *J. Climate,* **14,** 2238–2249.

Manabe, S., 1969: Climate and the ocean circulation. Part I: The atmospheric circulation and the hydrology of the earth's surface. *Mon. Wea. Rev.,* **97,** 739–774.

——, R. J. Stouffer, M. J. Spelman, and K. Bryan, 1991: Transient responses of a coupled ocean–atmosphere model to gradual changes of atmospheric CO2. Part I: Annual mean response. *J. Climate,* **4,** 785–818.

Mantua, N. J., S. R. Hare, Y. Zhang, J. M. Wallace, and R. C. Francis,

1997: A Pacific interdecadal climate oscillation with impacts on salmon production. *Bull. Amer. Meteor. Soc.*, **78,** 1069–1079.
Marotzke, J., and P. H. Stone, 1995: Atmospheric transports, the thermohaline circulation, and flux adjustments in a simple coupled model. *J. Phys. Oceanogr.,* **25,** 1350–1364.
Monahan, A. H., J. C. Fyfe, and G. M. Flato, 2000a: A regime view of Northern Hemisphere atmospheric variability and change under global warming. *Geophys. Res. Lett.,* **27,** 1139–1142.
——, L. Pandolfo, and J. C. Fyfe, 2000b: The preferred structure of variability of the Northern Hemisphere atmospheric circulation. *Geophys. Res. Lett.,* **28,** 1019–1022.
North, G. R., T. L. Bell, R. F. Cahalan, and F. J. Moeng, 1982: Sampling errors in the estimation of empirical orthogonal functions. *Mon. Wea. Rev.,* **110,** 699–706.
Palmer, T. N., 1999: A nonlinear dynamical perspective on climate prediction. *J. Climate,* **12,** 575–591.
Rogers, J. C., and H. van Loon, 1982: Spatial variability of sea level pressure and 500-mb height anomalies over the Southern Hemisphere. *Mon. Wea. Rev.,* **110,** 1375–1392.
Shindell, D. T., R. L. Miller, G. Schmidt, and L. Pandolfo, 1999: Simulation of recent northern winter climate trends by greenhouse-gas forcing. *Nature,* **399,** 452–455.
Silverman, B. W., 1986: *Density Estimation for Statistics and Data Analysis.* Chapman and Hall, 175 pp.
Stouffer, R. J., and S. Manabe, 1999: Response of a coupled ocean–atmosphere model to increasing atmospheric carbon dioxide: Sensitivity to the rate of increase. *J. Climate,* **12,** 2224–2237.
Thompson, D. W. J., and J. M. Wallace, 1998: The Arctic oscillation signature in the wintertime geopotential height and temperature fields. *Geophys. Res. Lett.,* **25,** 1297–1300.
——, and ——, 2000: Annular modes in the extratropical circulation. Part I: Month-to-month variability. *J. Climate,* **13,** 1000–1016.
Wallace, J. M., Y. Zhang, and L. Bayuk, 1996: Interpretation of interdecadal trends in Northern Hemisphere surface air temperature. *J. Climate,* **9,** 249–259.